Gravity-Induced Phase Transitions in the Standard Model and Beyond

Javier Rubio

Universidad Complutense de Madrid & IPARCOS

BUILDINGUNIVERSE

MINISTERIO DE CIENCIA E INNOVACIÓN

Fundación BBVA

The general paradigm

$$\frac{\mathcal{L}}{\sqrt{-g}} = \frac{M_P^2}{2} R - \frac{1}{2}(\partial\chi)^2 - f(R, R_{\mu\nu})\chi^2 - V(\chi)$$

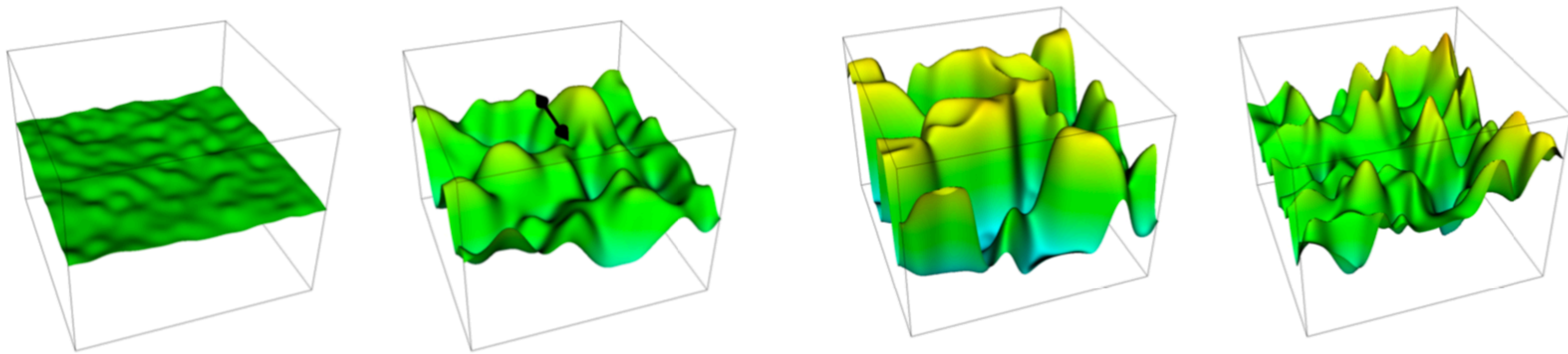

- Natural triggering mechanism for phase transitions
- Non-thermal & non-perturbative
- Short-lived topological defects
- Specific gravitational waves signatures

A dedicated program

1. Quintessential Affleck–Dine baryogenesis with non-minimal couplings,
   D. Bettoni, J. Rubio, Phys. Lett. B 784 (2018) 122–129.

2. Gravitational waves from global cosmic strings in quintessential inflation,
   D. Bettoni, G. Domènech, J. Rubio, JCAP 02 (2019) 034.

3. Hubble-induced phase transitions: Walls are not forever,
   D. Bettoni, J. Rubio, JCAP 01 (2020) 002.

4. Hubble-induced phase transitions on the lattice with applications to Ricci reheating,
   D. Bettoni, J. Rubio, JCAP 01 (2022) 002.

5. Ricci reheating reloaded,
   G. Laverda, JCAP 03 (2024) 033.

6. From Hubble to Bubble,
   M. Kierkla, G. Laverda, M. Lewicki, A. Mantziris, M. Piani, JHEP 11 (2023) 077.

7. The rise and fall of the Standard-Model Higgs: electroweak vacuum stability during kination,
   G. Laverda, J. Rubio, JHEP 05 (2024) 339.

8. Tachyonic gravitational dark matter production after inflation,
   G. Laverda, T, Mendes, J. Rubio, arxiv:2601.XXXX

The SM Higgs tracker

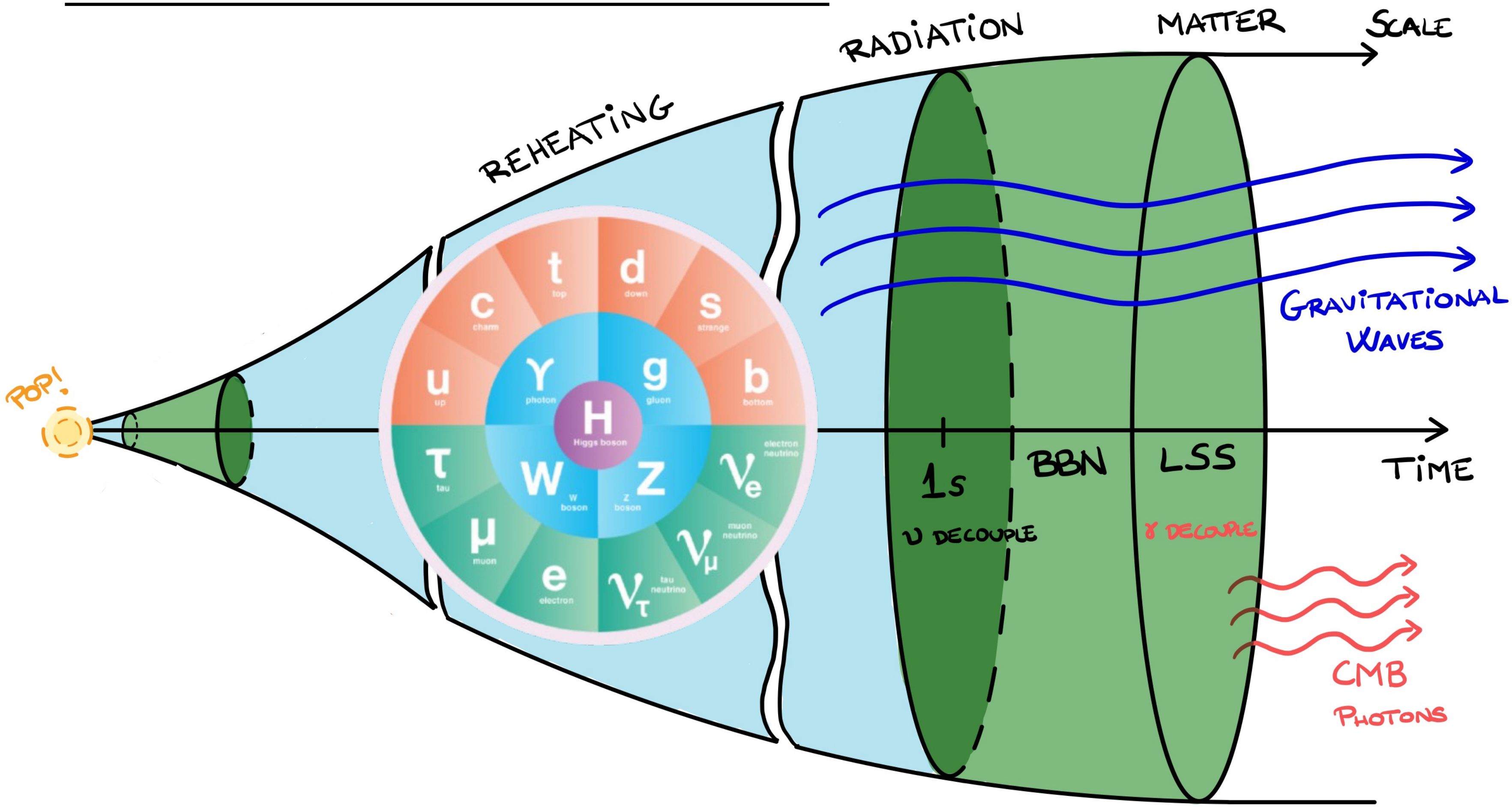

$$\Delta\mathcal{L}_{\rm SM+G} = \sqrt{-g}\,\xi H^\dagger H\, g^{\mu\nu} R_{\mu\nu}(\Gamma)$$

Sensitive to cosmological history

A simple scenario

- A single field ϕ for both inflation and dark energy (quintessential inflation)
- An unavoidable non-minimal coupling of the Higgs field H to gravity
- No additional degrees of freedom beyond the electroweak scale

$$\frac{\mathcal{L}}{\sqrt{-g}} = \frac{M_{\rm P}^2}{2}R - g^{\mu\nu}(D_\mu H)^\dagger(D_\nu H) - \lambda\left(H^\dagger H - \frac{v_{\rm EW}^2}{2}\right)^2 - \xi H^\dagger H R + \mathcal{L}_{\rm SM} + \mathcal{L}_\phi$$

Interesting outputs

- The Higgs field is safely stabilized during inflation (no isocurvature pert.)
- Appealing connection between SM parameters and (post-)inflationary era
- The Higgs field itself can be responsible for heating the Universe

G. Laverda, JR, JCAP 03 (2024) 033 & JHEP 05 (2024) 339

Quintessential inflation

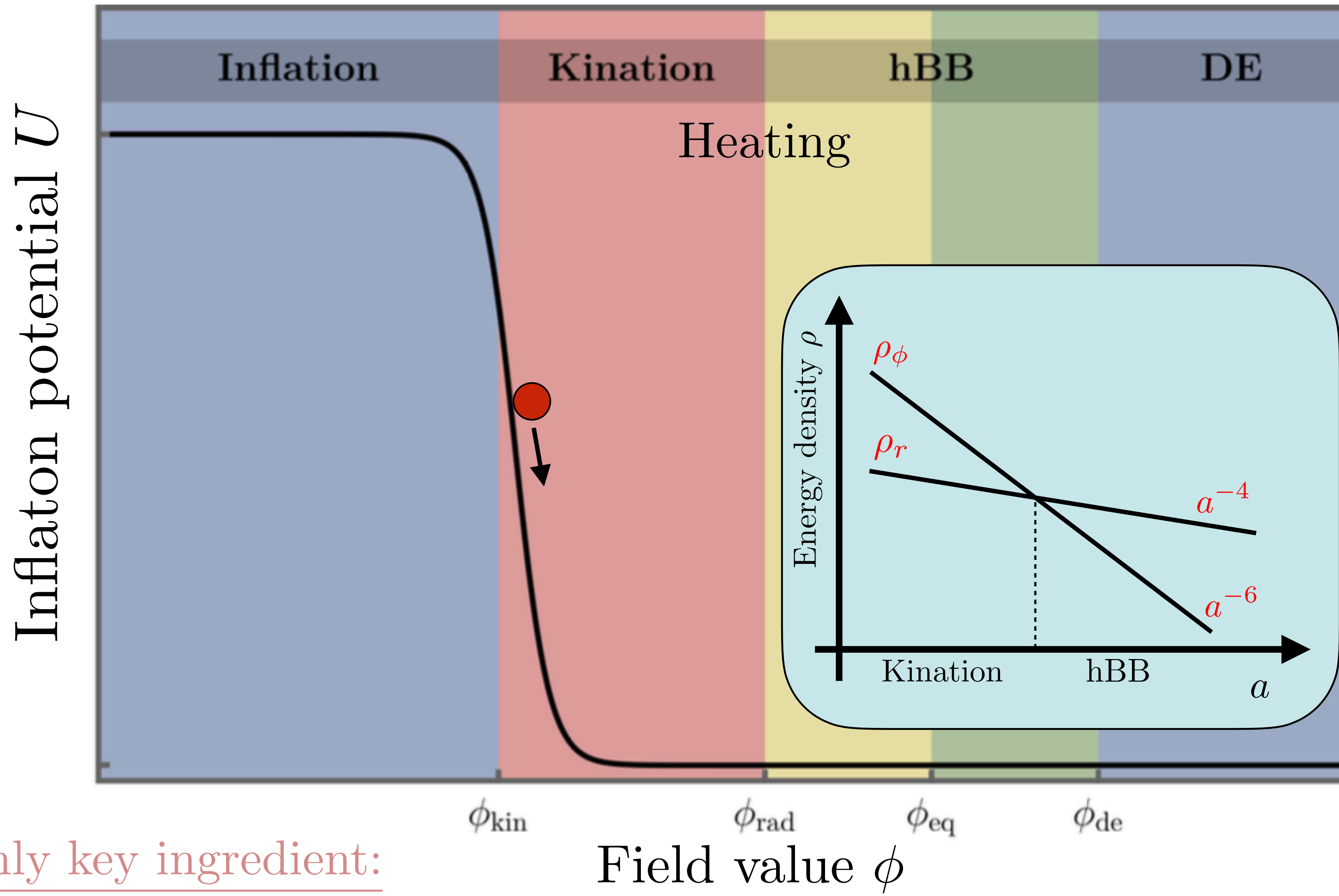

Only key ingredient:

Period of kination

For a review see e.g. D. Bettoni, JR, Galaxies 10 (2022) 1, 22

Hubble-induced transition

$$V_{\text{eff}}(H) = (\xi R + m_h^2) H^\dagger H + \lambda (H^\dagger H)^2$$

Energetically subdominant / Spectator field $R = 3(1 - 3w_\phi)\mathcal{H}^2$

Negligible contribution to the effective Planck mass, $\xi h^2 \ll M_P^2$

Inflation $w_\phi = -1$ Kination $w_\phi = 1$

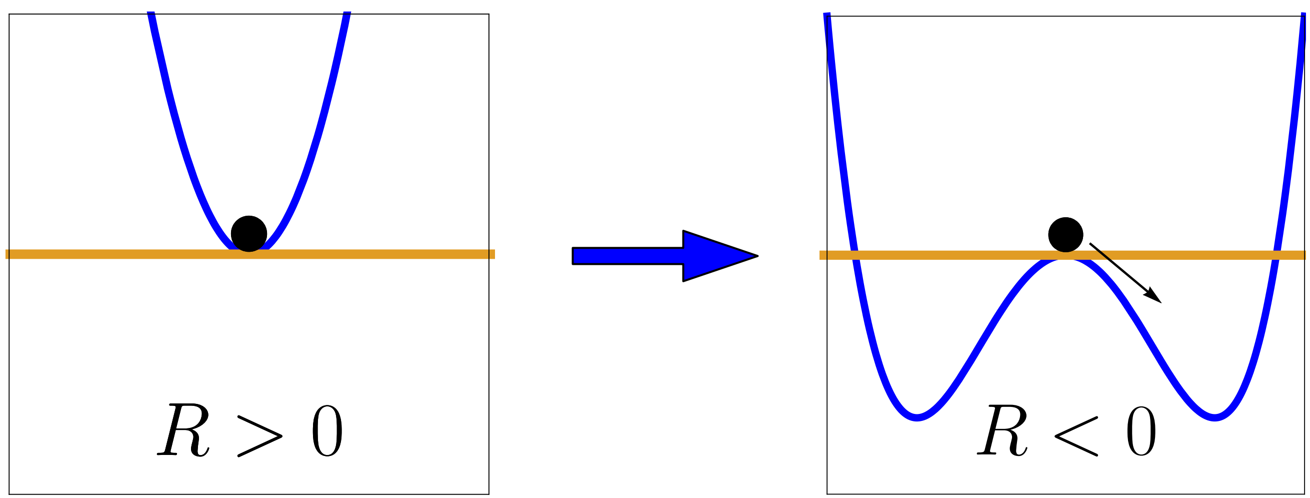

No isocurvature perturbations Tachyonic production

Standard Model running

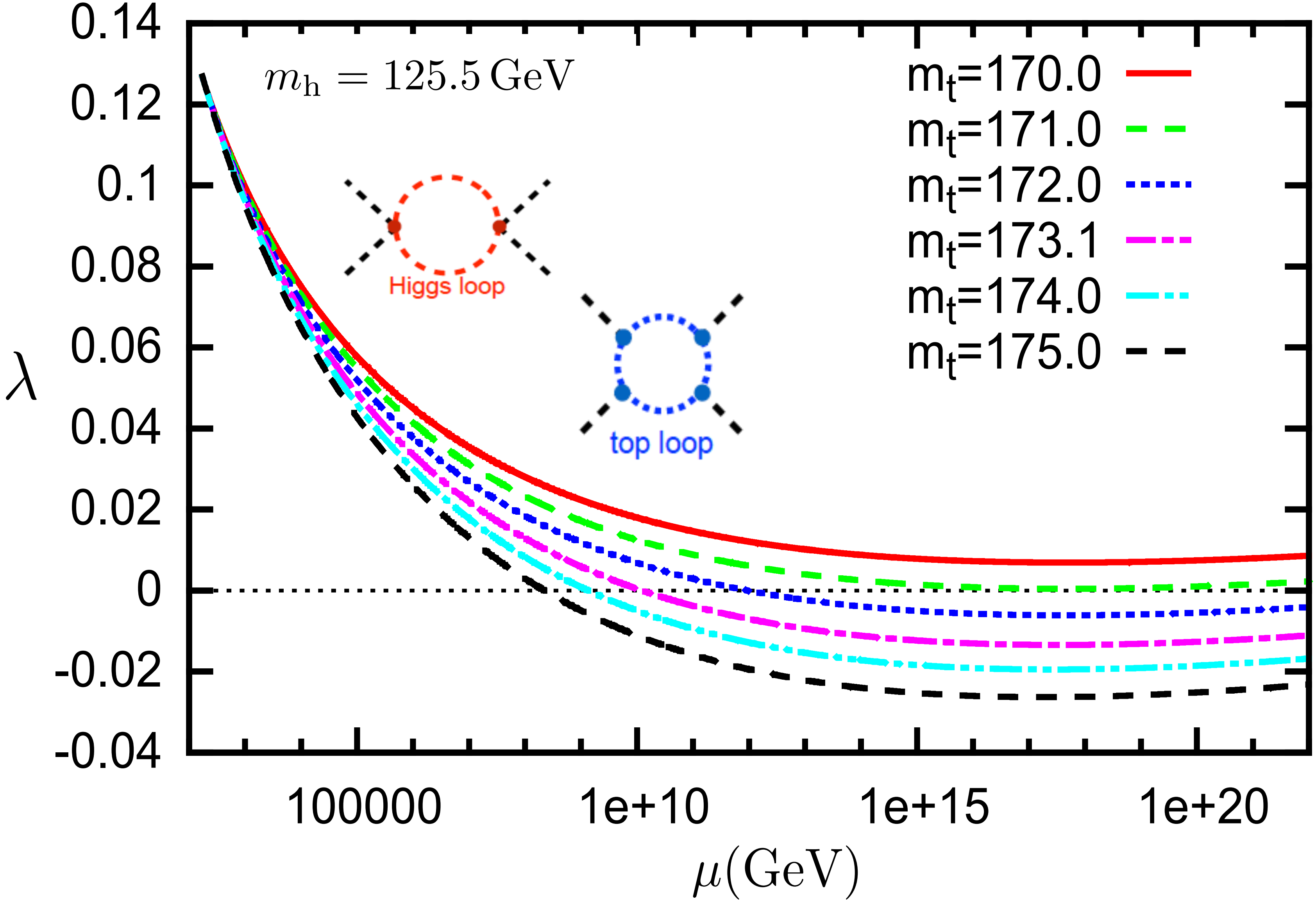

Higgs effective potential

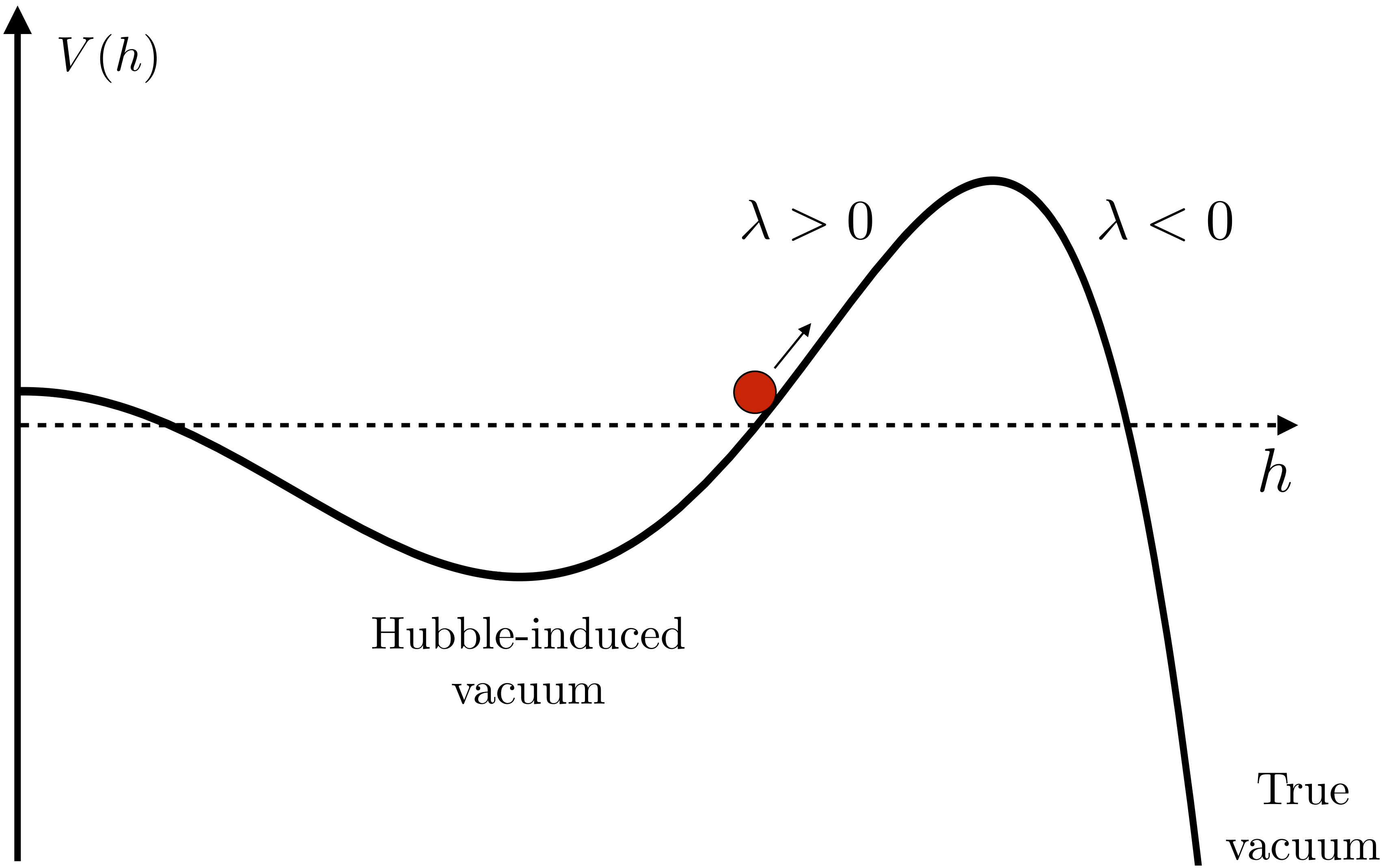

Classicalization

- The field is *not* classical but rather quantum.
- A homogeneous component description is *completely inaccurate*.

$$f''_\kappa + (\kappa^2 - M^2_{\text{eff}}(z))f_\kappa = 0$$

$$F_\kappa(z) = \mathrm{Re}(f^*_\kappa f'_\kappa)$$

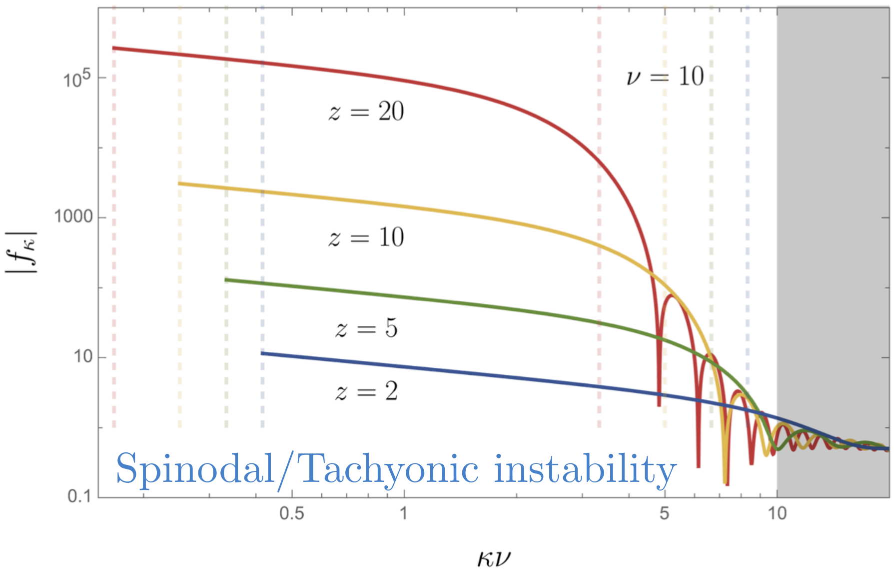

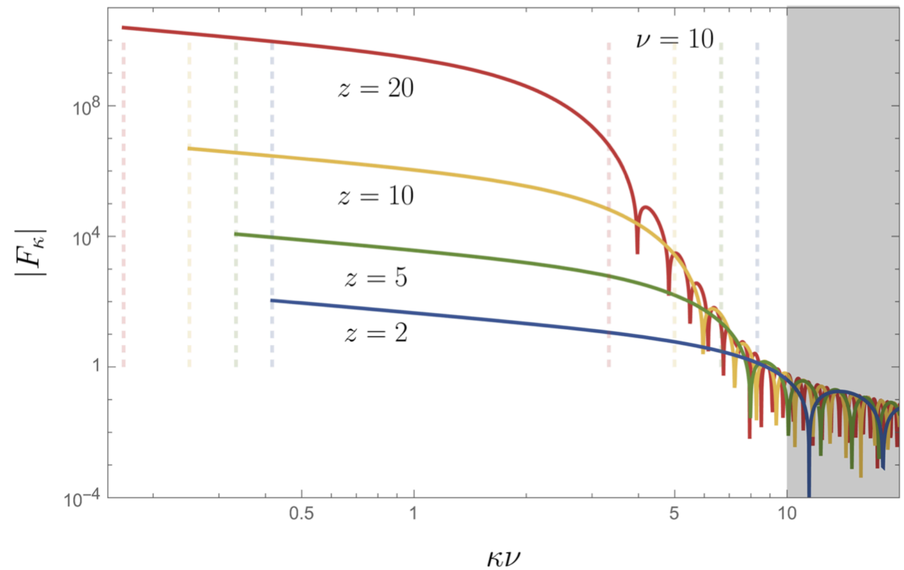

$$\Delta Y^2_\kappa \, \Delta\Pi^2_\kappa = |F_\kappa(z)|^2 + \frac{1}{4} \geq \frac{1}{4}\left|\langle[Y_\kappa(z),\ \Pi^\dagger_\kappa(z)]\rangle\right|^2$$

- Following dynamics needs non-analytical techniques.
- High occupation numbers → Classical Lattice Simulations

D. Bettoni, JR, JCAP 01 (2020) 002

Scanning of parameter space

- Three-loop renormalisation-group running of the Higgs self-coupling
- Agnostic approach to top quark mass values, $m_t = 170 - 173$ GeV
- Wide range for non-minimal coupling parameter $\xi \sim 1 - 700$
- Wide range for the onset scale of kination $\mathcal{H}_{\rm kin} \sim 10^6 - 10^{15}$ GeV
- O(1000) 3+1-dimensional classical lattice simulations.
- Checking for existence and crossing of the barrier

$$\xi < \frac{y_\Lambda^4 \mu_\Lambda^2}{32\, e^{3/2} \pi^2\, \mathcal{H}^2}$$

$$\rho_{\rm tac}(\lambda(\mu), \xi) < V(h_{\rm max}(\xi, y_\Lambda, \mathcal{H}, \mu_\Lambda))$$

Heating the Universe before BBN

Explosive tachyonic Higgs production allows to heat the Universe.

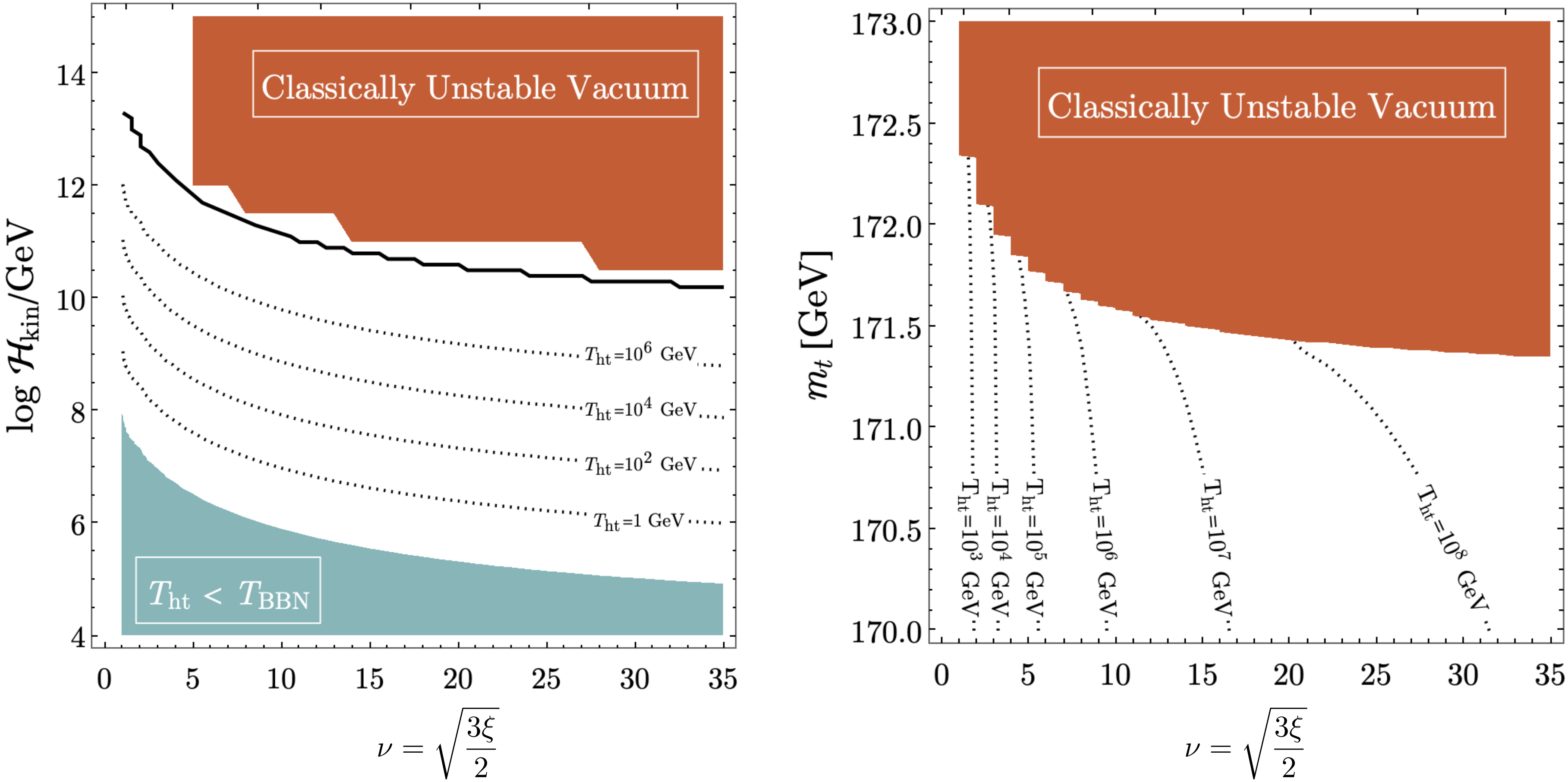

$\mathcal{H}_{\rm kin} = 10^{10}$ GeV

Lower bound on the inflationary scale
Favours lower masses for the top quark

G. Laverda, JR, JHEP 05 (2024) 339

Gradients are large!

$$(h_{ij}^{TT})'' + 2H(h_{ij}^{TT})' - \frac{\nabla^2 h_{ij}^{TT}}{a^2} \simeq \frac{2a^2}{M_P^2}\Pi_{ij}^{TT}$$

$$\Pi_{ij} = \partial_i\chi\partial_j\chi - \xi\partial_i\partial_j\chi^2$$

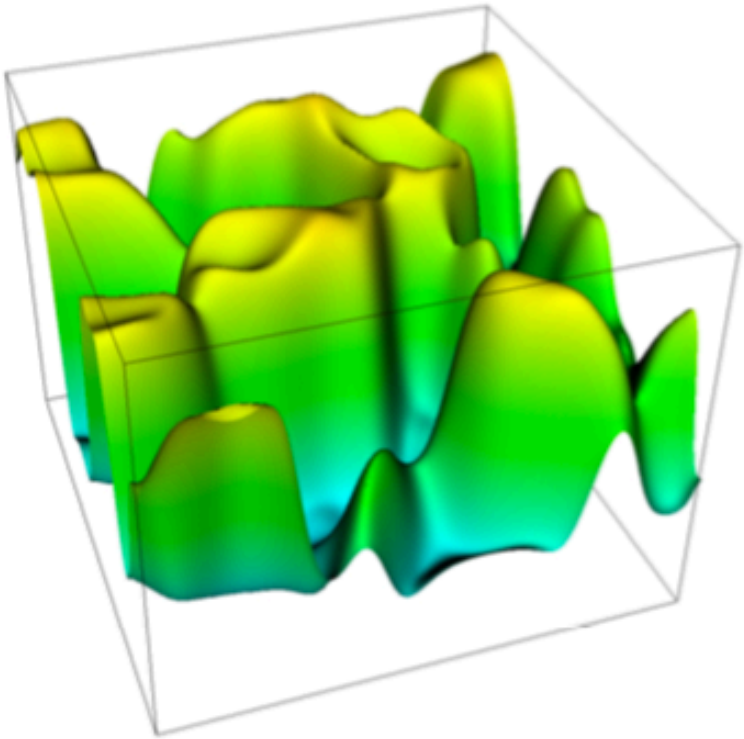

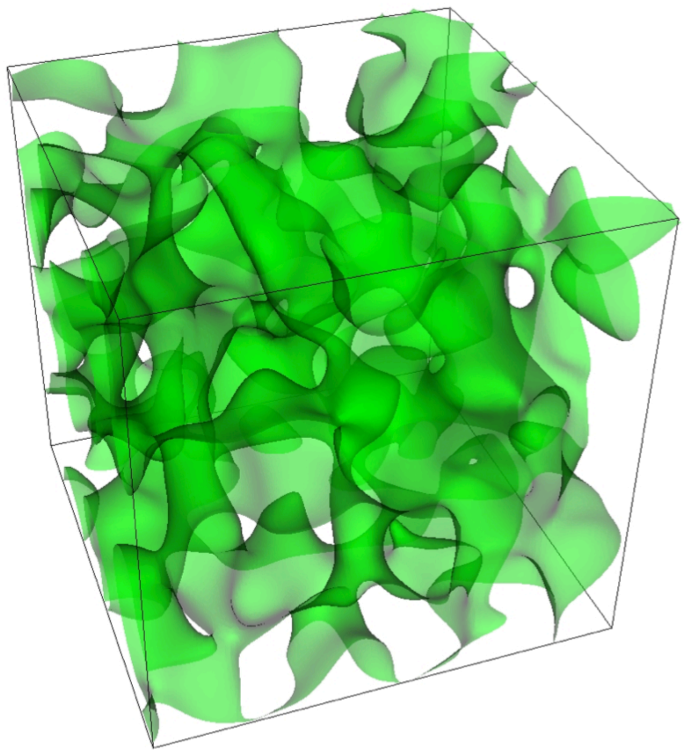

D. Bettoni, G. Domènech, J. Rubio, JCAP 02 (2019) 034

D. Bettoni, A López-Eiguren, G. Laverda, JR, JCAP 03 (2025) 027

GW energy density

$$\Omega_{\mathrm{GW},0}(\mathcal{H}_{\mathrm{kin}}, \nu, m_t) = 1.67 \times 10^{-5} h^{-2} \left(\frac{100}{g_*^{\mathrm{ht}}}\right)^{1/3} \times \bar{\Omega}_{\mathrm{GW}}$$

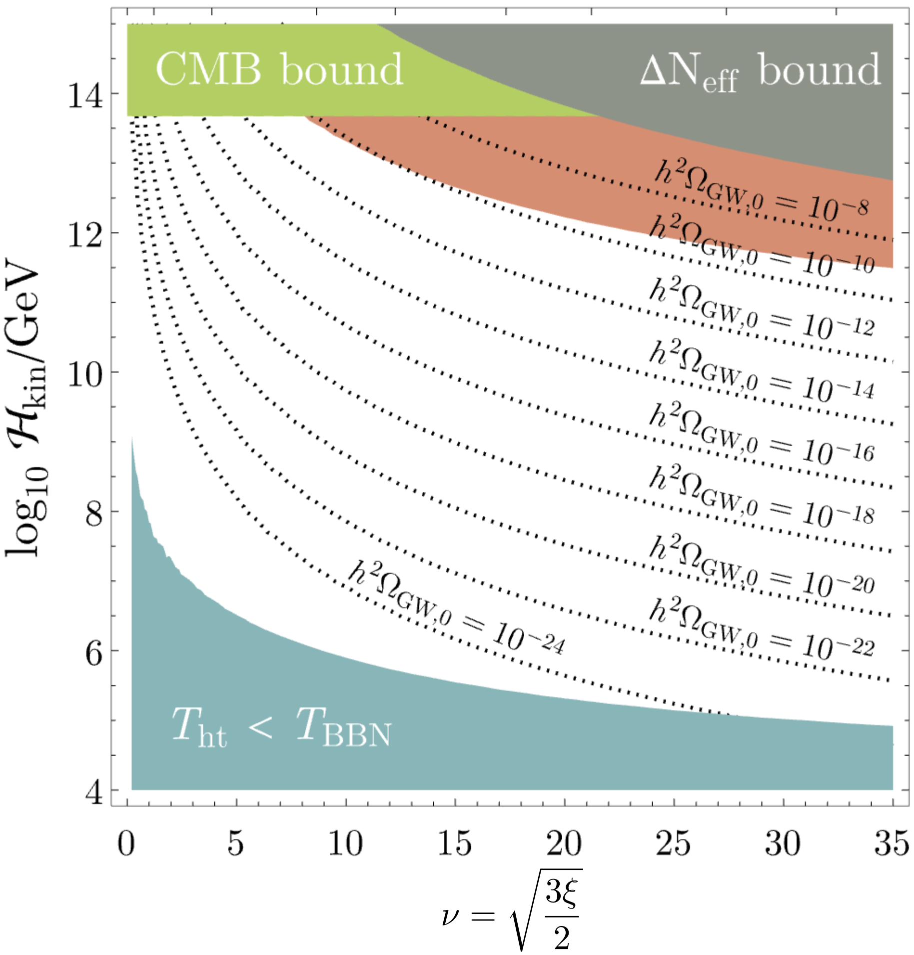

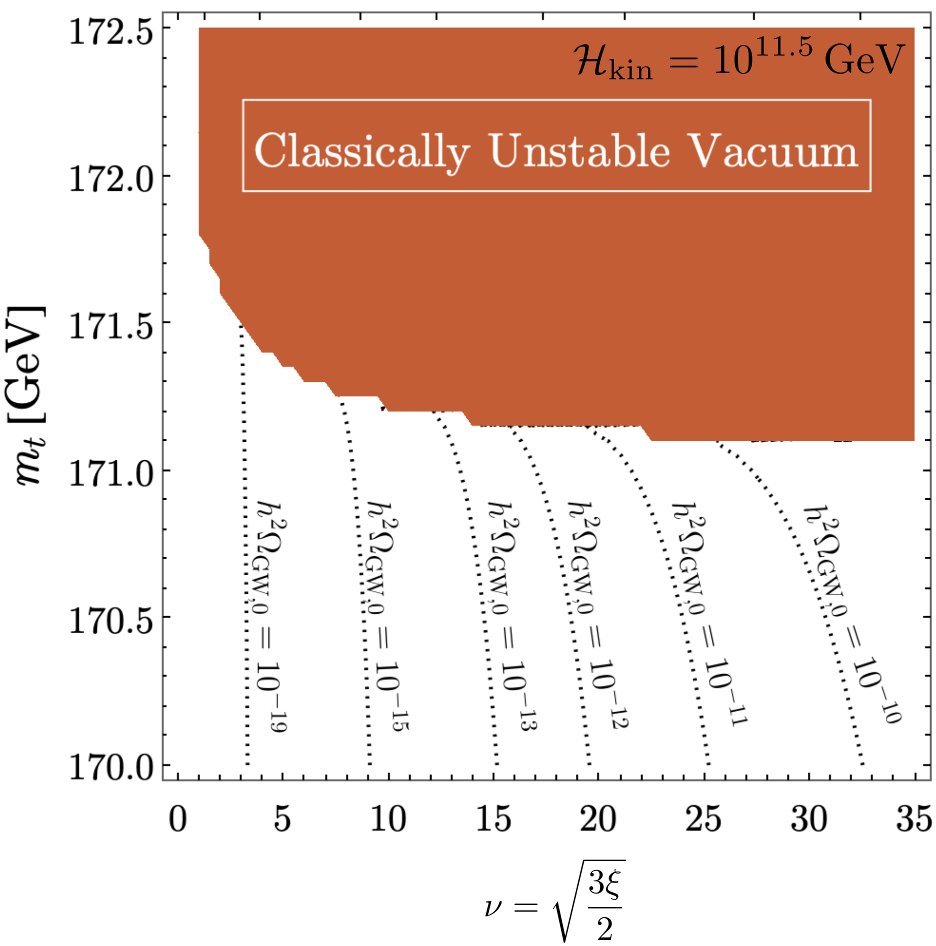

GW spectra

$$\bar{\Omega}_{\rm GW}(\mathcal{H}_{\rm kin}, \nu, m_t; f) = \frac{\bar{\Omega}_{\rm p}(a+b)^c}{\left[a\left(\frac{f}{f_{\rm p}}\right)^{b/c} + b\left(\frac{f}{f_{\rm p}}\right)^{-a/c}\right]^c},$$

$$a = 3.00\,, \qquad b = 152.34 - 6.57\,\nu\,, \qquad c = 105.85 - 4.79\,\nu\,.$$

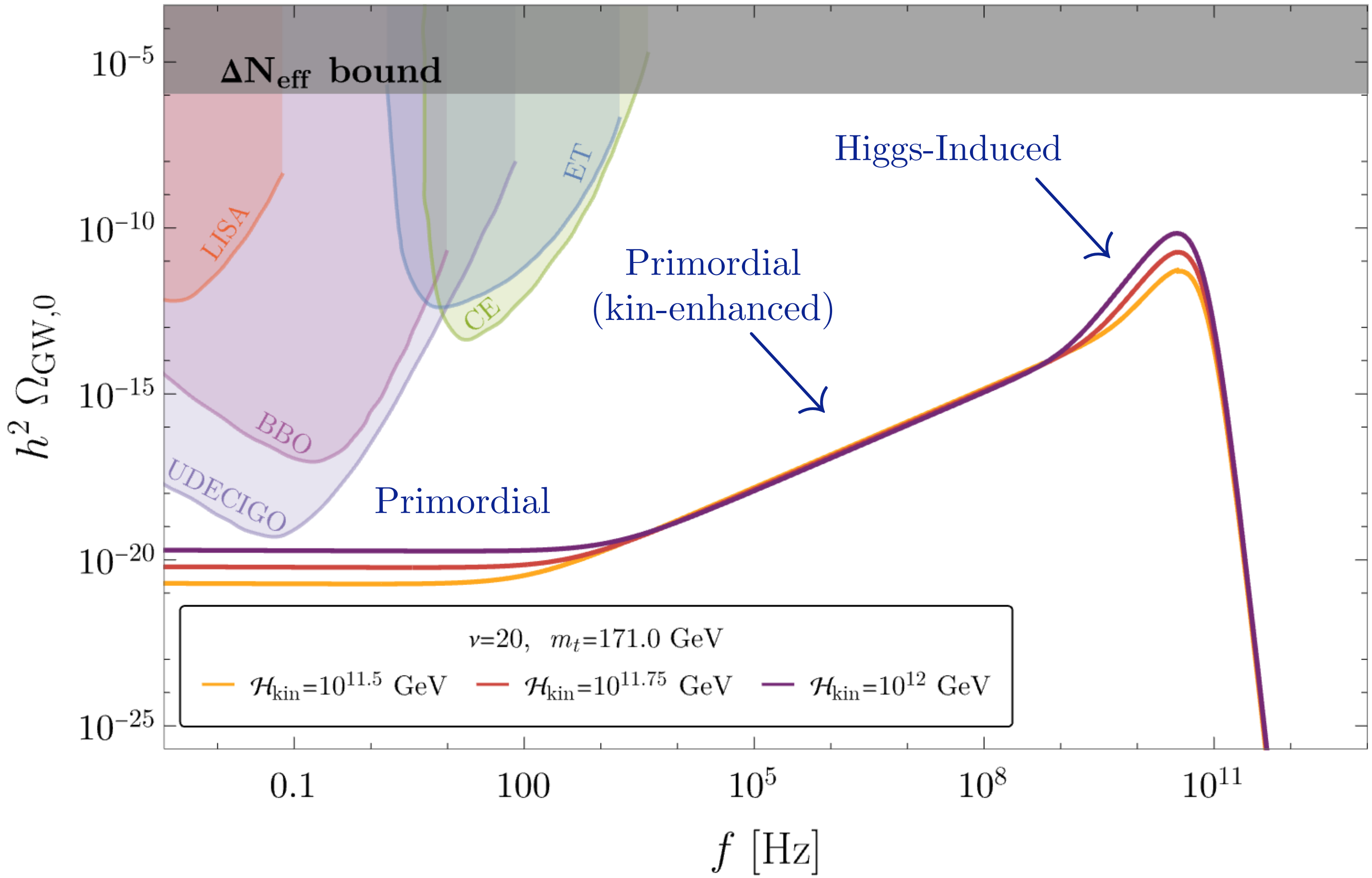

Beyond kination: Gravitational EFT

$$\frac{\Delta\mathcal{L}}{\sqrt{-g}} = -\frac{1}{2}\xi R\chi^2 - \left(\alpha R^2 + \beta R_{\mu\nu}R^{\mu\nu} + \gamma R_{\mu\nu\rho\sigma}R^{\mu\nu\rho\sigma}\right)\frac{\chi^2}{\Lambda^2} + \ldots$$

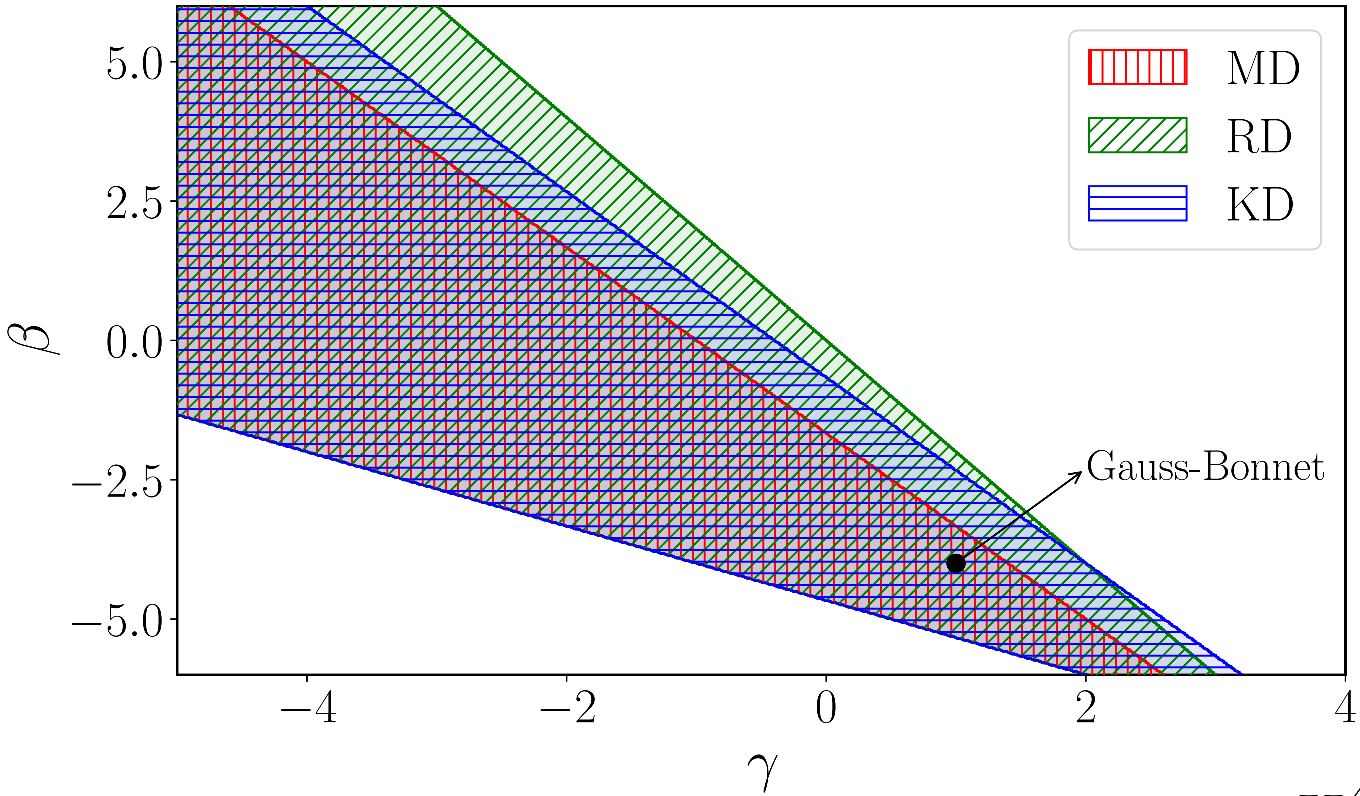

$$M_{\text{eff}}^2 = M^2 + 3\xi(1-3w)H^2 + C(\alpha,\beta,\gamma,\omega)\frac{H^4}{\Lambda^2}$$

Higher-order operators may become relevant during radiation domination

Conclusions

- Time-dependent spacetime curvature can trigger phase transitions via Hubble-induced instabilities.
- Specific cosmological transitions (e.g. inflation $\rightarrow$ kination) naturally destabilize the Higgs and other spectator fields.
- This mechanism enables efficient reheating before BBN without requiring direct couplings to new sectors.
- It predicts distinctive high-frequency gravitational-wave signatures.

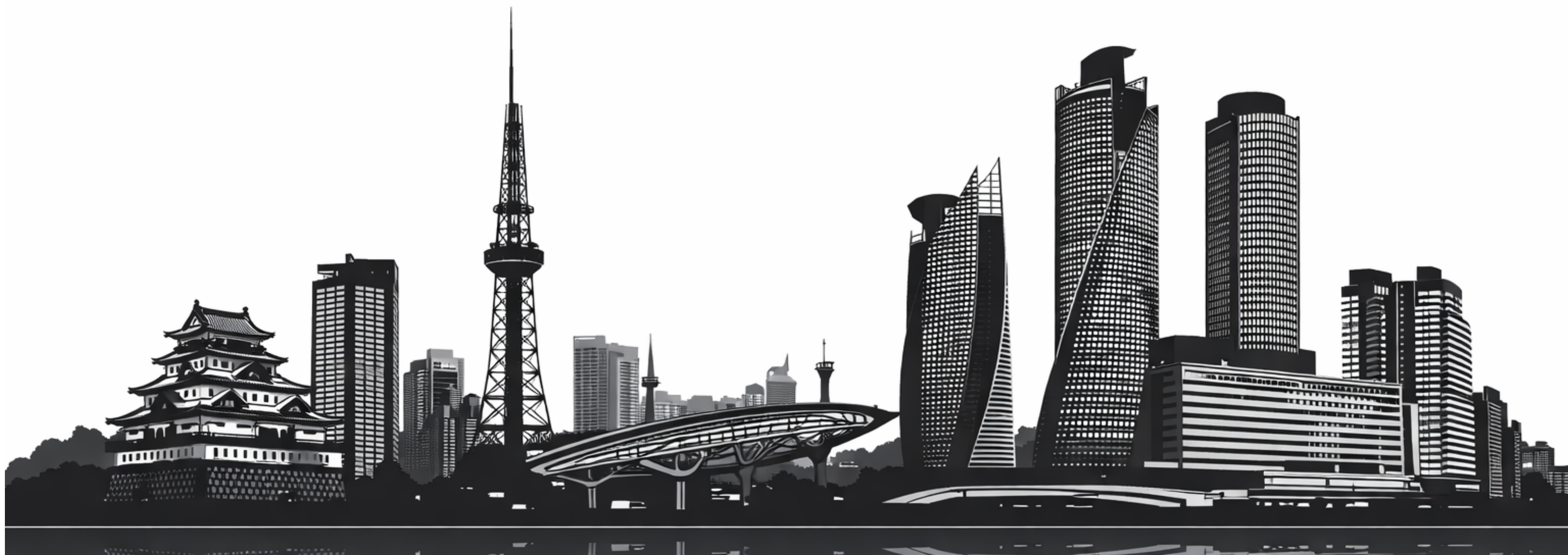

Backup slides

Tachyonic particle production

$$Y \equiv \frac{a}{a_{\rm kin}}\frac{h}{h_*} \qquad \vec{y} \equiv a_{\rm kin} h_* \vec{x} \qquad h_* \equiv \sqrt{6\xi} H_{\rm kin}$$
$$z \equiv a_{\rm kin} h_* \tau$$

Spinodal/Tachyonic instability

$$S_\chi = \int d^3\vec{y}\, dz \left[\frac{1}{2}(Y')^2 - \frac{1}{2}|\nabla Y|^2 + \frac{1}{2}M^2_{\rm eff}(z)Y^2 - \cancel{V(Y)}\right]$$

$$M^2_{\rm eff}(z) \equiv (4\nu^2 - 1)\mathcal{H}^2 \qquad \nu \equiv \sqrt{\frac{3\xi}{2}}$$

- The field is *not* classical but rather quantum.
- A homogeneous component description is *completely inaccurate.*

D. Bettoni, JR, JCAP 01 (2020) 002

Energy distribution

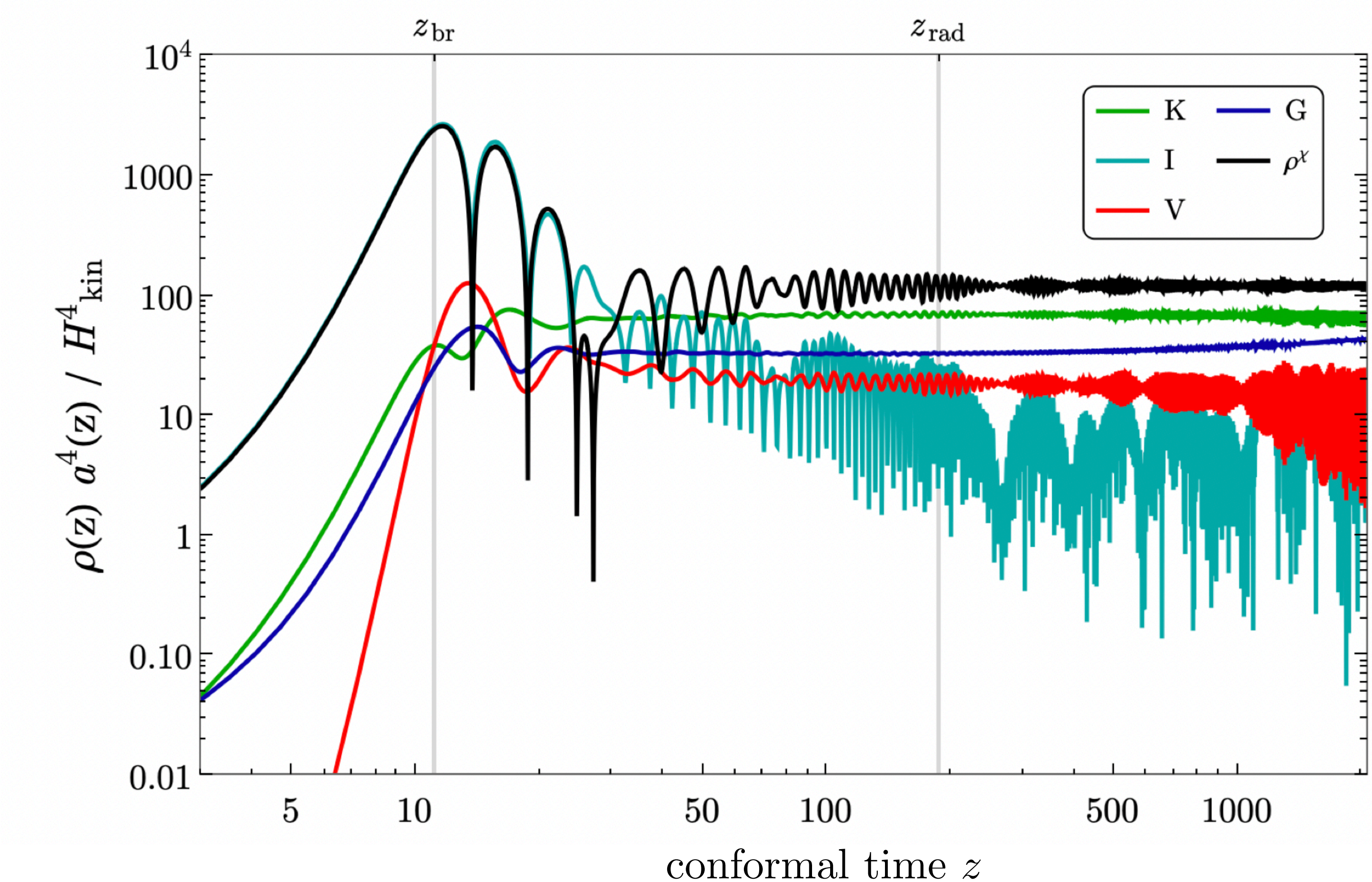

Lattice-based fitting formulas: O(100) 3+1 classical lattice simulations

$$\rho_{\rm tac}(\lambda(\mu), \xi) = 16\, \mathcal{H}^4_{\rm kin}\ \exp\left(\beta_1(\lambda) + \beta_2(\lambda)\, \nu + \beta_3(\lambda) \ln \nu\right) \qquad \nu = \sqrt{\frac{3\xi}{2}}$$

G. Laverda, JR, JCAP 03 (2024) 033

Gradients are crucial

G. Laverda, JR, JCAP 03 (2024) 033

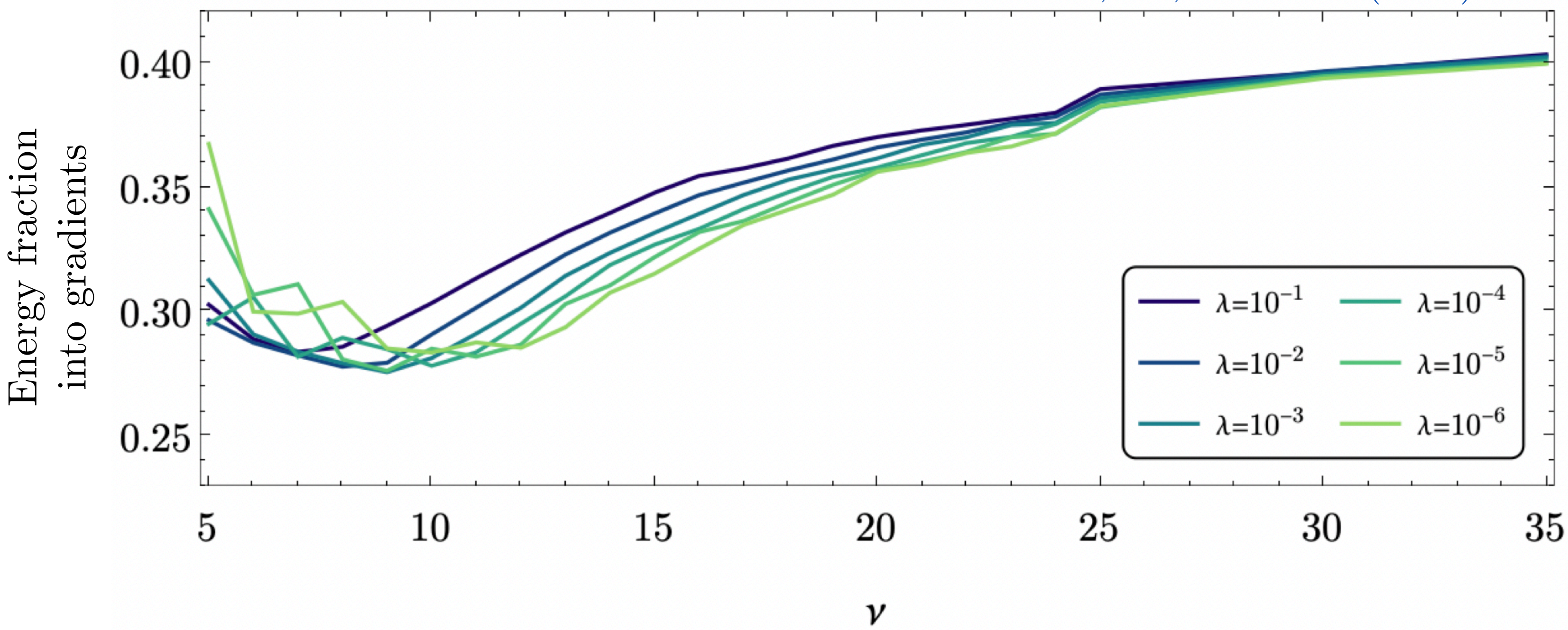

Radiation-like products for arbitrary potential

$$w_\chi = \frac{1}{3} + \frac{2}{3}\frac{(n-2)}{(n+1) + \langle(\nabla\chi/a)^2\rangle/\langle V\rangle} \qquad V \propto \chi^{2n}$$

D.Bettoni, A. Lopez-Eiguren, JR, JCAP 01 (2022) 01, 002

Onset of radiation domination

Lattice-based fitting formulas: O(100) 3+1 classical lattice simulations

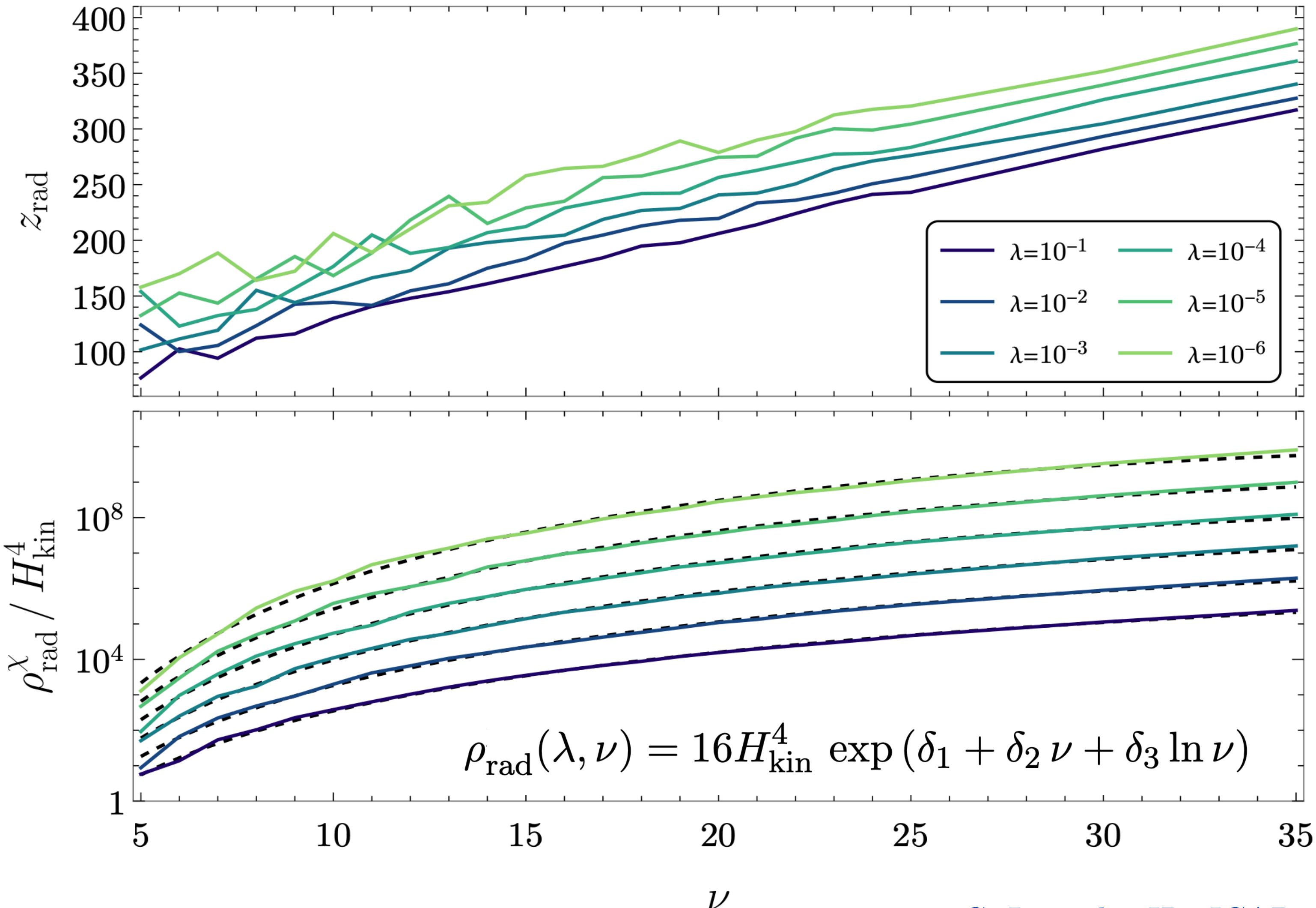

G. Laverda, JR, JCAP 03 (2024) 033

Heating "temperature"

By-product
First lattice characterisation
of Ricci reheating

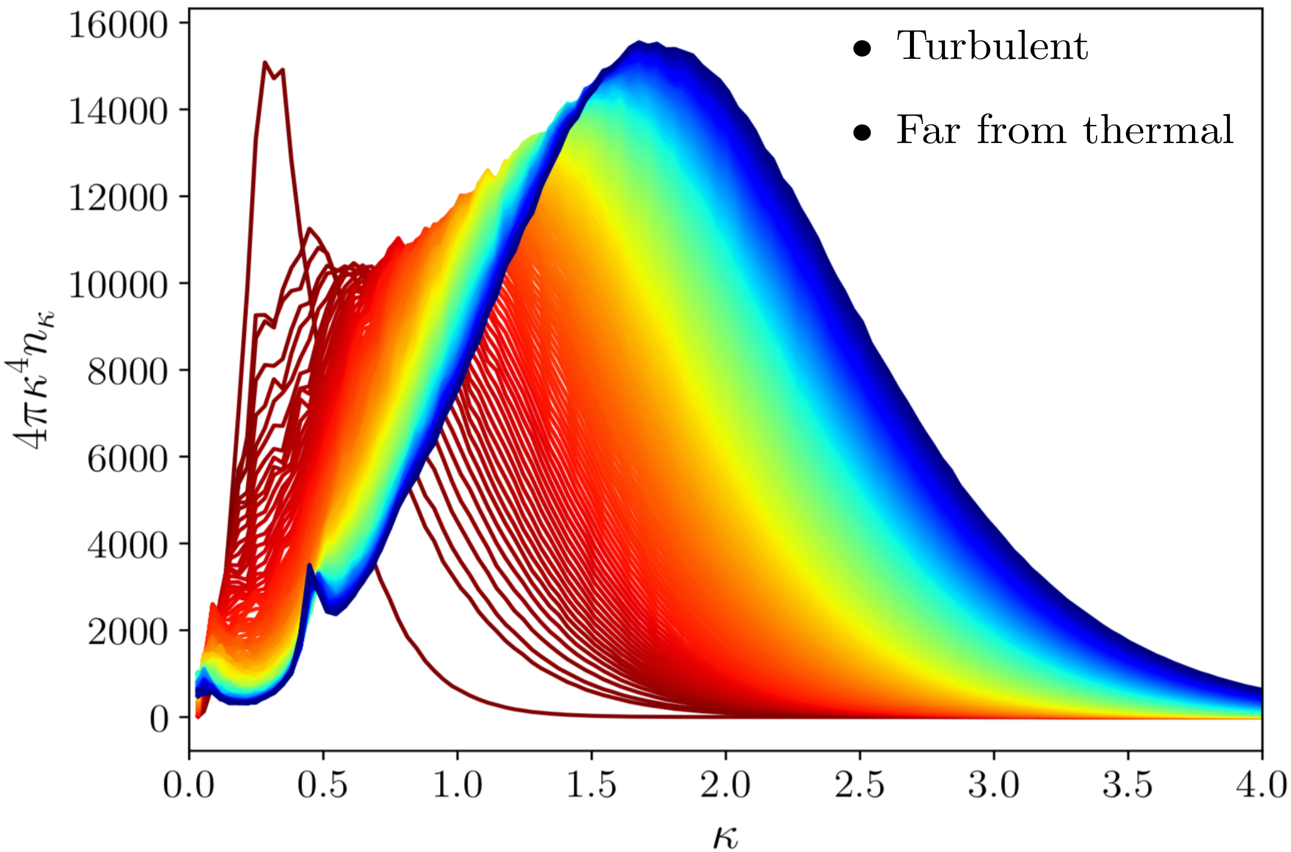

$$T_{\rm ht} \simeq 2.7 \times 10^8\,\text{GeV} \left(1 + \frac{z_{\rm rad}}{\nu}\right)^{-3/4} \left(\frac{\rho_{\rm rad}/\rho^{\phi}_{\rm rad}}{10^{-8}}\right)^{3/4} \left(\frac{H_{\rm kin}}{10^{11}\,\text{GeV}}\right)^{1/2}$$

D.Bettoni, A. Lopez-Eiguren, JR, JCAP 01 (2022) 01, 002
G. Laverda, JR, JCAP 03 (2024) 033

Vacuum stability during kination

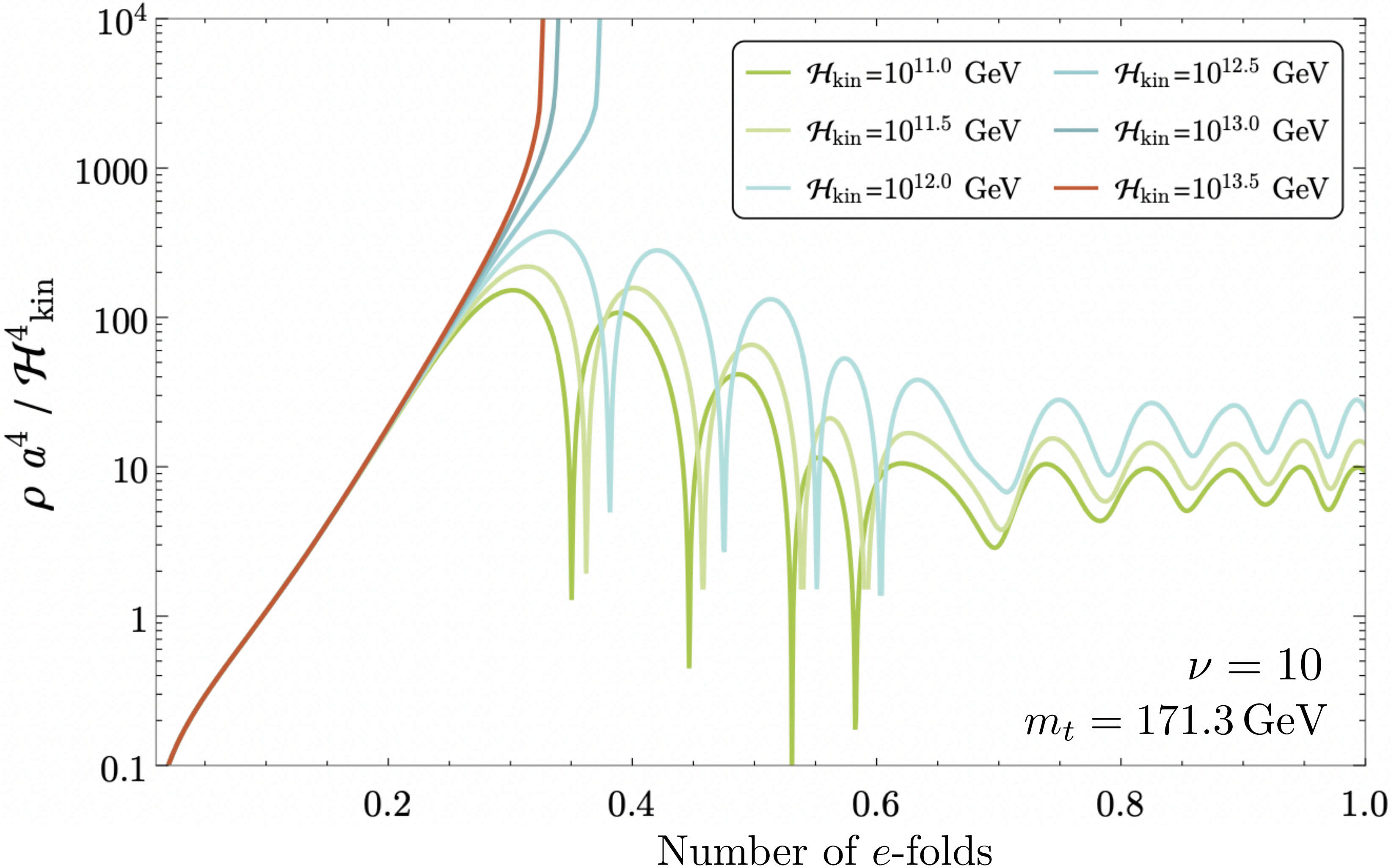

G. Laverda, JR, 2402.06000

GW frequency

$$f_{\mathrm{GW},0}(\nu, m_t) \simeq 1.3 \times 10^9 \,\mathrm{Hz}\, \frac{\kappa}{2\pi} \left(\frac{\mathcal{H}_{\mathrm{kin}}\, a_{\mathrm{rad}}}{10^{10}\ \mathrm{GeV}}\right)^{1/2} \left(\frac{\Theta^h_{\mathrm{ht}}}{10^{-8}}\right)^{-1/4}$$

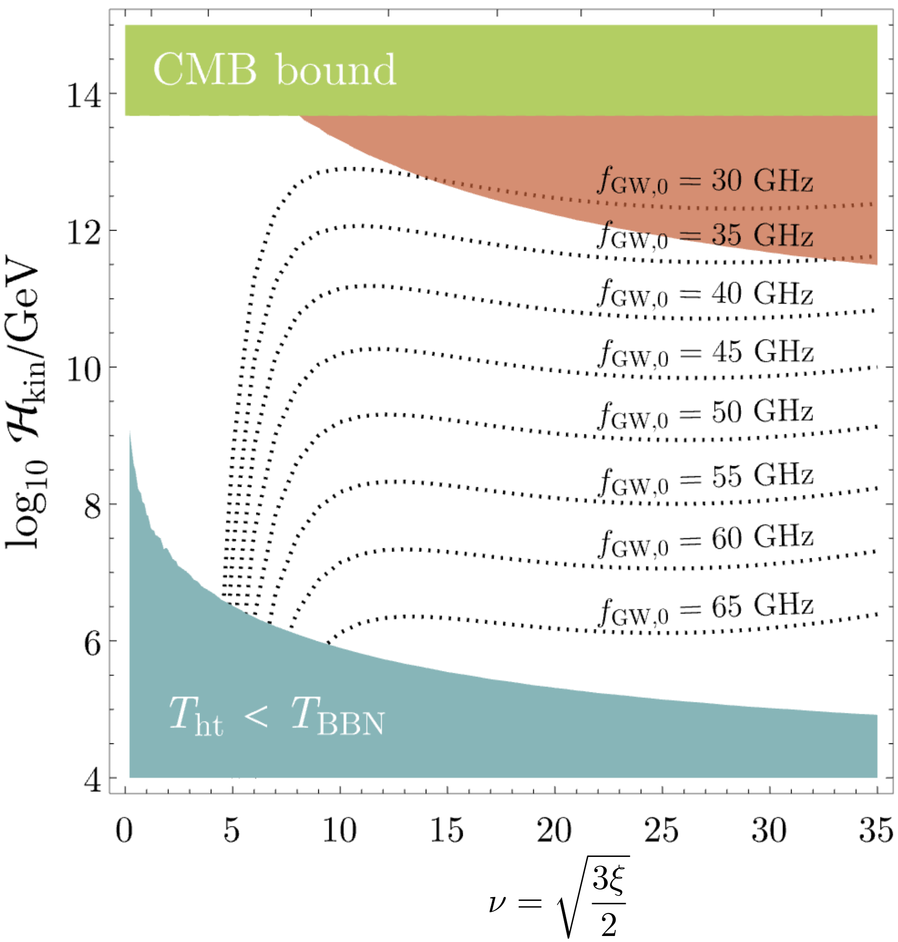

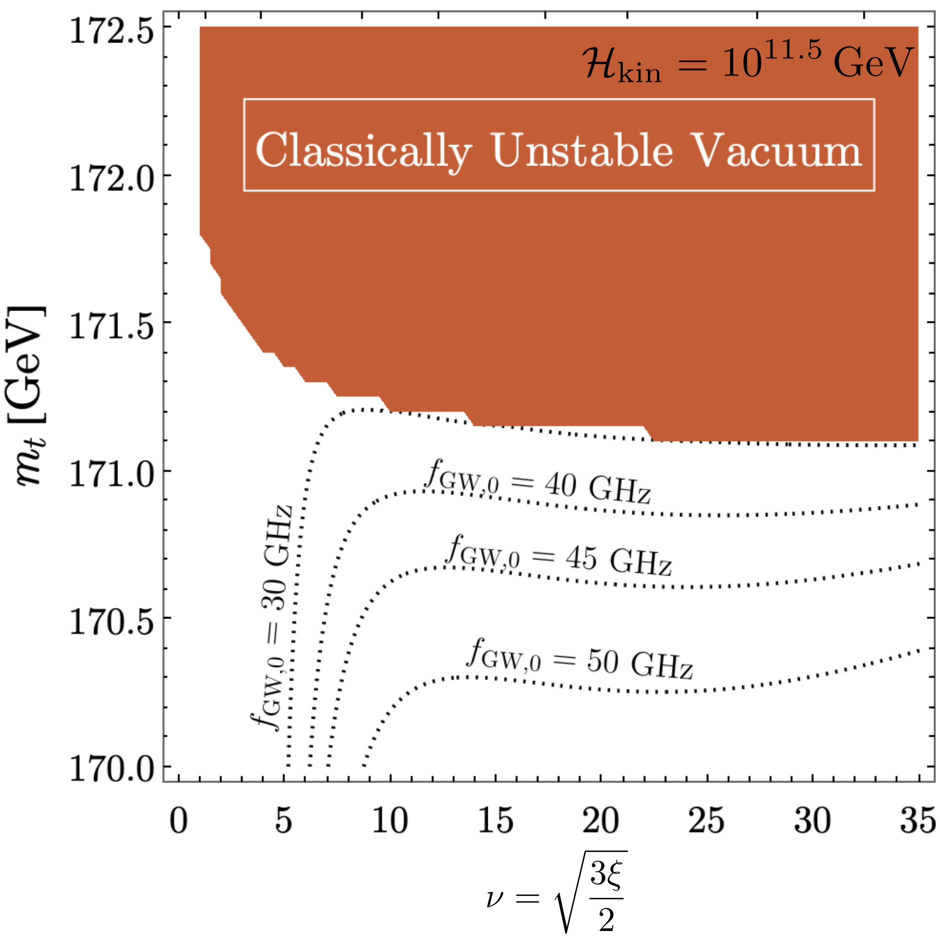

Beyond the Standard Model

$$V_{\text{eff}}(H) = (\xi R + m_h^2) H^\dagger H + \lambda (H^\dagger H)^2 + \frac{1}{\Lambda^2}(H^\dagger H)^3$$

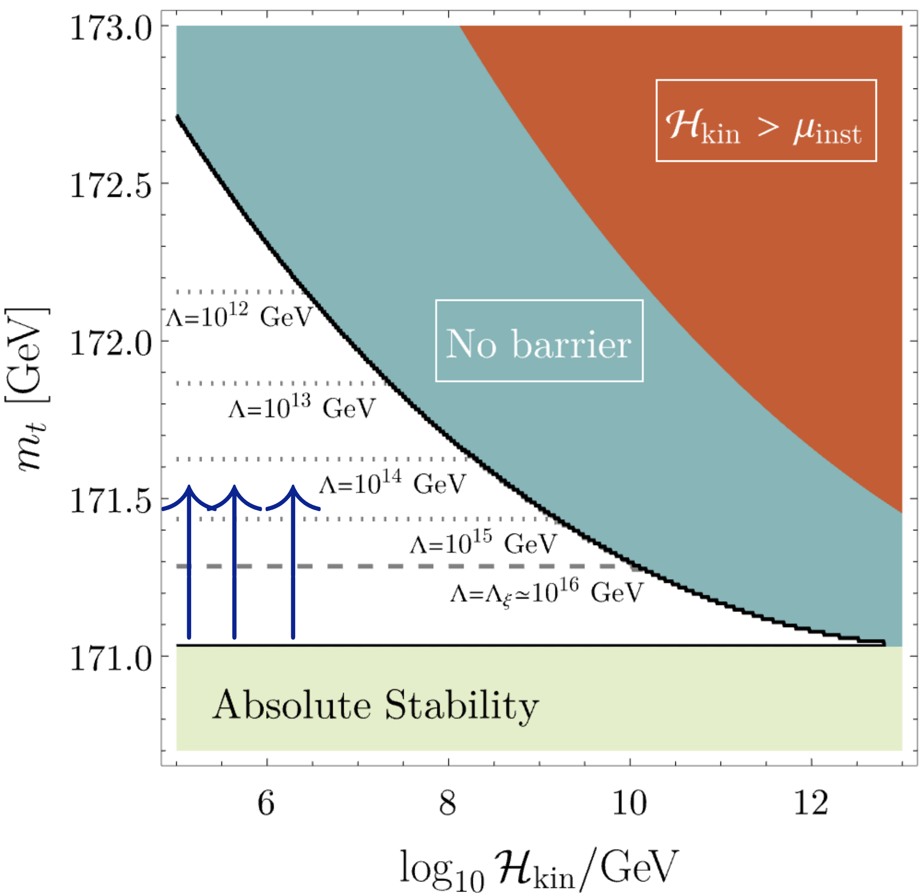

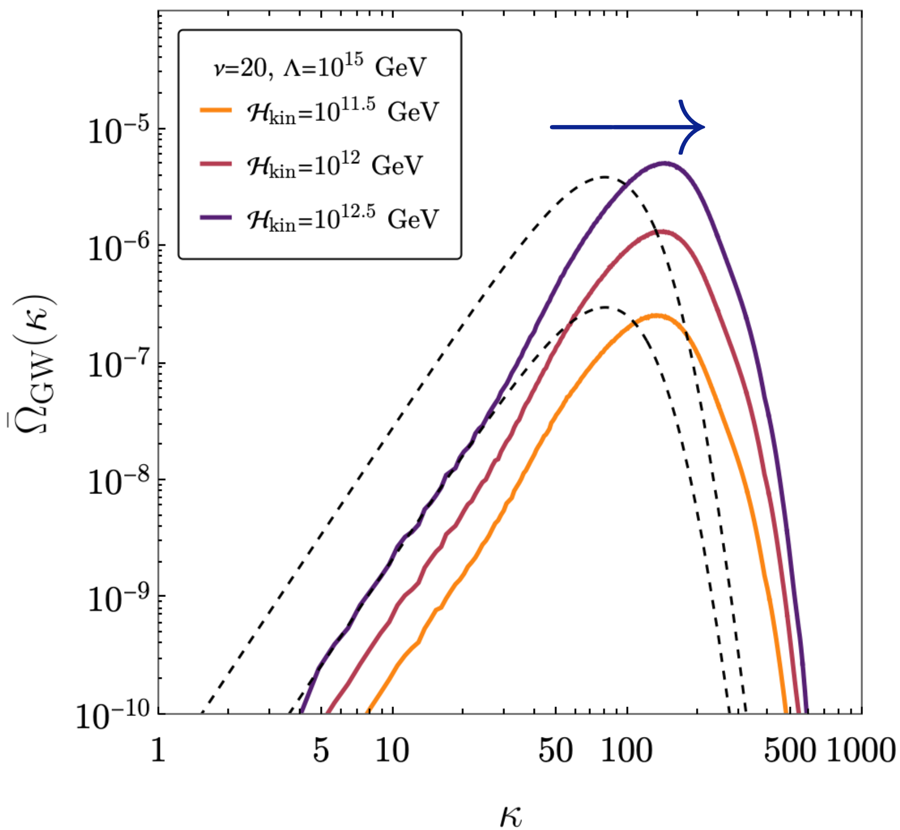

Stability constraints on the top mass

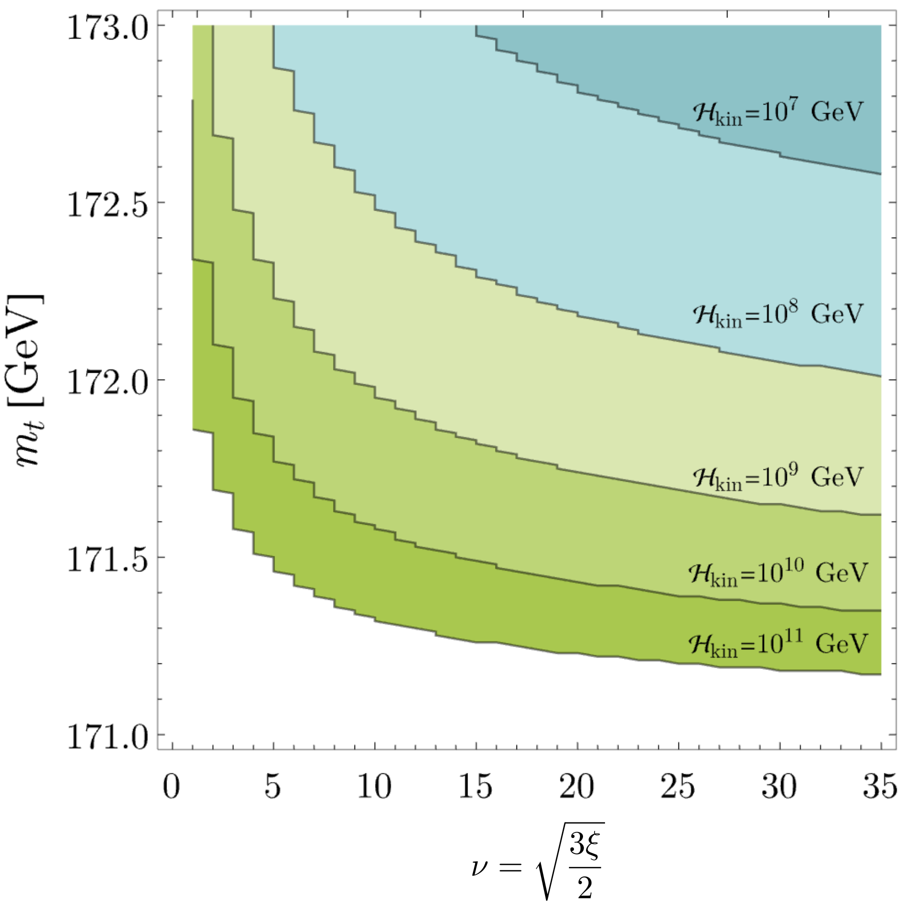

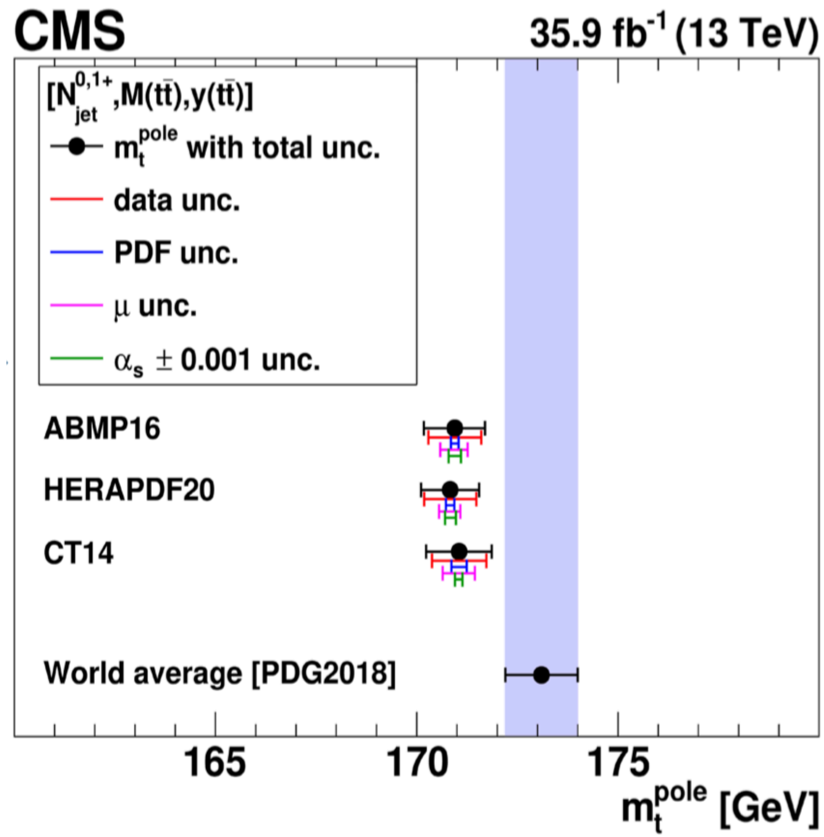

Favours lower masses for the top quark

G. Laverda, JR, JHEP 05 (2024) 339

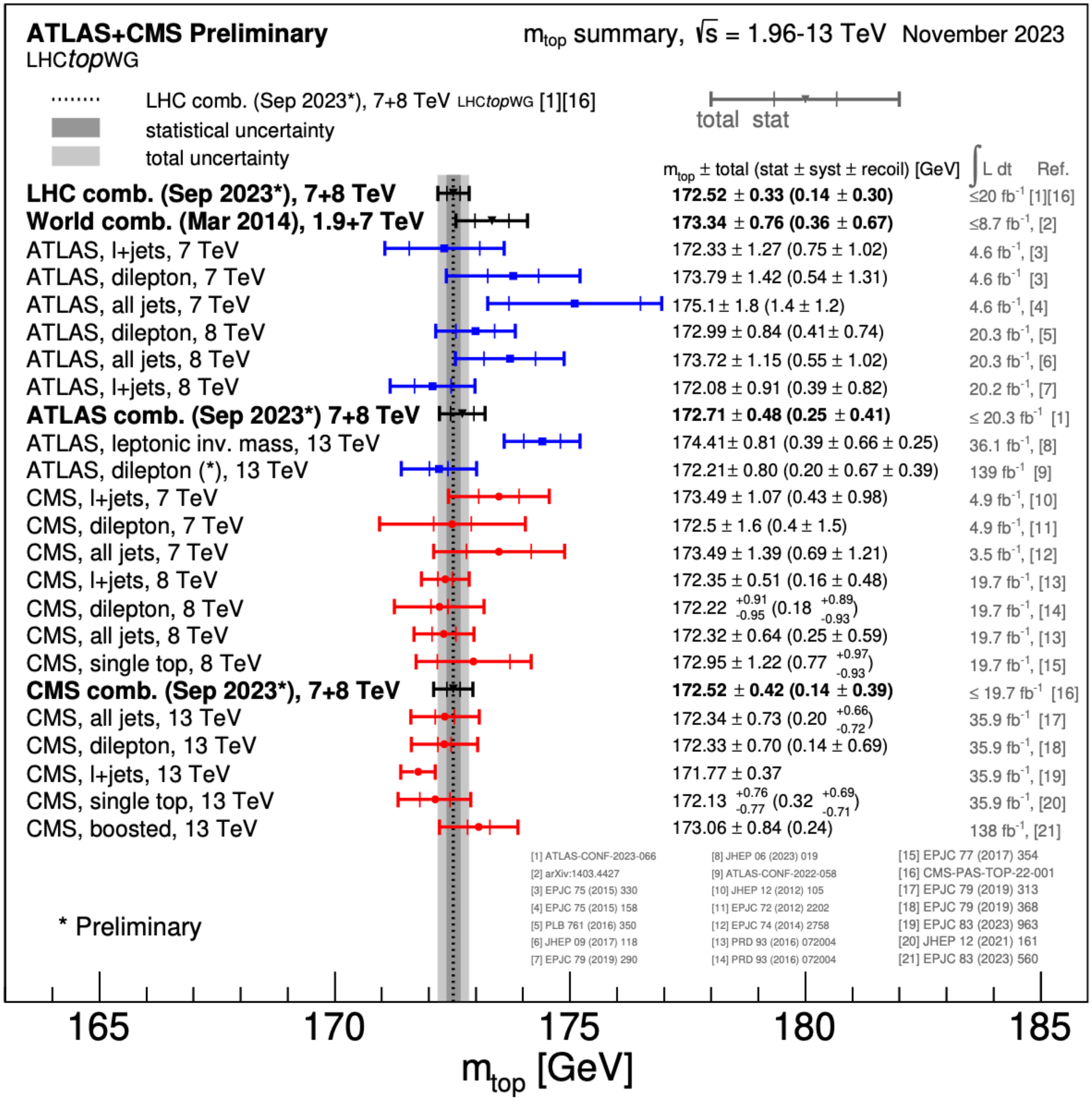

ATLAS+CMS Preliminary
LHCtopWG
m_top summary, √s = 1.96-13 TeV November 2023
LHC comb. (Sep 2023*), 7+8 TeV LHCtopWG [1][16]
statistical uncertainty
total uncertainty
total stat
m_top ± total (stat ± syst ± recoil) [GeV]
∫L dt
Ref.
LHC comb. (Sep 2023*), 7+8 TeV
172.52 ± 0.33 (0.14 ± 0.30)
≤20 fb^-1 [1][16]
World comb. (Mar 2014), 1.9+7 TeV
173.34 ± 0.76 (0.36 ± 0.67)
≤8.7 fb^-1, [2]
ATLAS, l+jets, 7 TeV
172.33 ± 1.27 (0.75 ± 1.02)
4.6 fb^-1, [3]
ATLAS, dilepton, 7 TeV
173.79 ± 1.42 (0.54 ± 1.31)
4.6 fb^-1 [3]
ATLAS, all jets, 7 TeV
175.1 ± 1.8 (1.4 ± 1.2)
4.6 fb^-1, [4]
ATLAS, dilepton, 8 TeV
172.99 ± 0.84 (0.41 ± 0.74)
20.3 fb^-1, [5]
ATLAS, all jets, 8 TeV
173.72 ± 1.15 (0.55 ± 1.02)
20.3 fb^-1, [6]
ATLAS, l+jets, 8 TeV
172.08 ± 0.91 (0.39 ± 0.82)
20.2 fb^-1, [7]
ATLAS comb. (Sep 2023*) 7+8 TeV
172.71 ± 0.48 (0.25 ± 0.41)
≤ 20.3 fb^-1 [1]
ATLAS, leptonic inv. mass, 13 TeV
174.41 ± 0.81 (0.39 ± 0.66 ± 0.25)
36.1 fb^-1, [8]
ATLAS, dilepton (*), 13 TeV
172.21 ± 0.80 (0.20 ± 0.67 ± 0.39)
139 fb^-1 [9]
CMS, l+jets, 7 TeV
173.49 ± 1.07 (0.43 ± 0.98)
4.9 fb^-1, [10]
CMS, dilepton, 7 TeV
172.5 ± 1.6 (0.4 ± 1.5)
4.9 fb^-1, [11]
CMS, all jets, 7 TeV
173.49 ± 1.39 (0.69 ± 1.21)
3.5 fb^-1, [12]
CMS, l+jets, 8 TeV
172.35 ± 0.51 (0.16 ± 0.48)
19.7 fb^-1, [13]
CMS, dilepton, 8 TeV
172.22 +0.91 -0.95 (0.18 +0.89 -0.93)
19.7 fb^-1, [14]
CMS, all jets, 8 TeV
172.32 ± 0.64 (0.25 ± 0.59)
19.7 fb^-1, [13]
CMS, single top, 8 TeV
172.95 ± 1.22 (0.77 +0.97 -0.93)
19.7 fb^-1, [15]
CMS comb. (Sep 2023*), 7+8 TeV
172.52 ± 0.42 (0.14 ± 0.39)
≤ 19.7 fb^-1 [16]
CMS, all jets, 13 TeV
172.34 ± 0.73 (0.20 +0.66 -0.72)
35.9 fb^-1 [17]
CMS, dilepton, 13 TeV
172.33 ± 0.70 (0.14 ± 0.69)
35.9 fb^-1, [18]
CMS, l+jets, 13 TeV
171.77 ± 0.37
35.9 fb^-1, [19]
CMS, single top, 13 TeV
172.13 +0.76 -0.77 (0.32 +0.69 -0.71)
35.9 fb^-1, [20]
CMS, boosted, 13 TeV
173.06 ± 0.84 (0.24)
138 fb^-1, [21]
[1] ATLAS-CONF-2023-066
[2] arXiv:1403.4427
[3] EPJC 75 (2015) 330
[4] EPJC 75 (2015) 158
[5] PLB 761 (2016) 350
[6] JHEP 09 (2017) 118
[7] EPJC 79 (2019) 290
[8] JHEP 06 (2023) 019
[9] ATLAS-CONF-2022-058
[10] JHEP 12 (2012) 105
[11] EPJC 72 (2012) 2202
[12] EPJC 74 (2014) 2758
[13] PRD 93 (2016) 072004
[14] PRD 93 (2016) 072004
[15] EPJC 77 (2017) 354
[16] CMS-PAS-TOP-22-001
[17] EPJC 79 (2019) 313
[18] EPJC 79 (2019) 368
[19] EPJC 83 (2023) 963
[20] JHEP 12 (2021) 161
[21] EPJC 83 (2023) 560
* Preliminary
165
170
175
180
185
m_top [GeV]

An open question

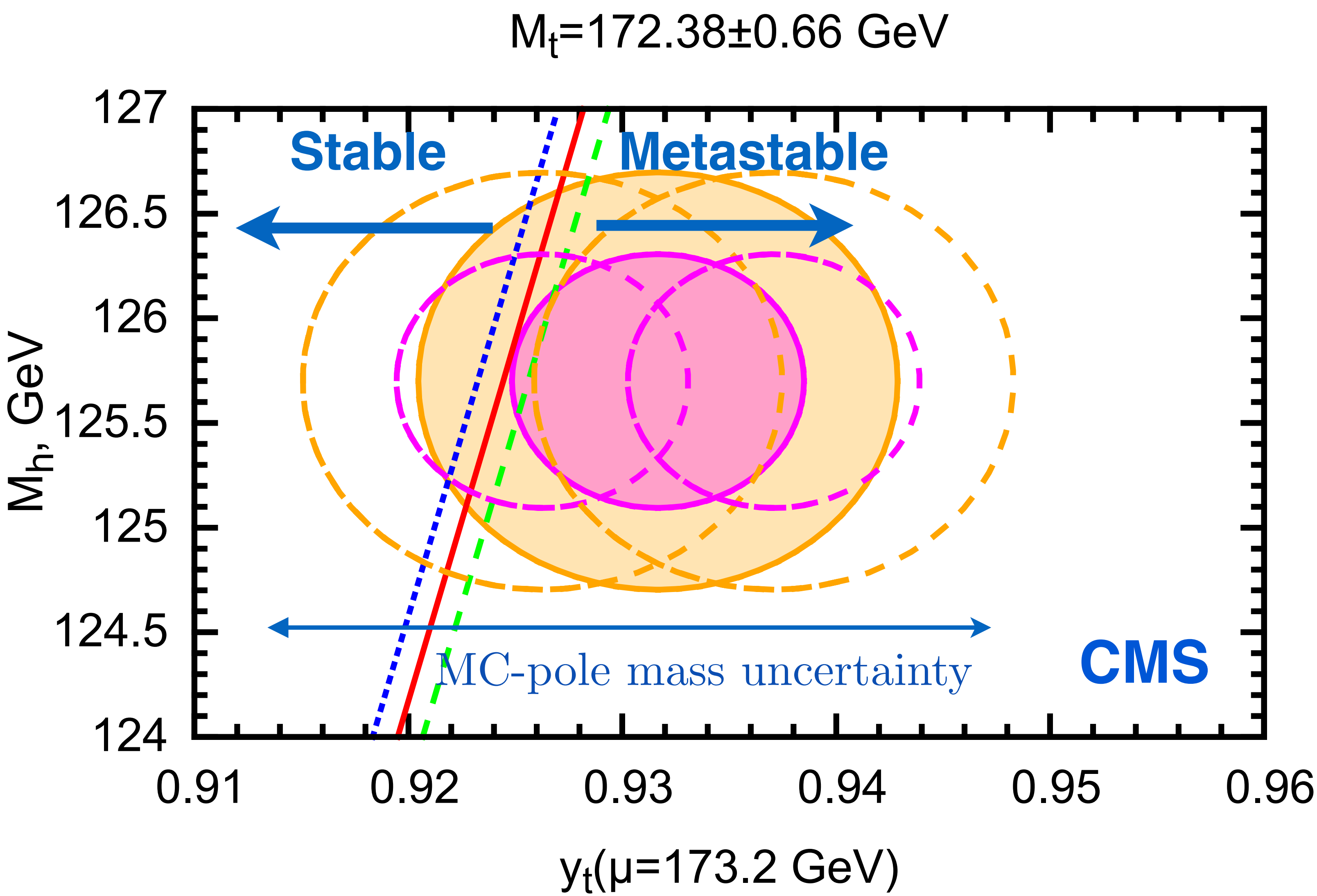

F. Bezrukov, M. Shaposhnikov, J.Exp.Theor.Phys. 120 (2015) 335-343,